Disproportionation and Other Transformations of N₂O at High Pressures and Temperatures to Lower Energy, Denser Phases

C. S. Yoo,[†] V. Iota,[†] H. Cynn,[†] M. Nicol,*,[‡] J. H. Park,[†] T. Le Bihan,[§] and M. Mezouar[§]

Lawrence Livermore National Laboratory, Livermore, California 94551, High-Pressure Science and Engineering Center, University of Nevada Las Vegas, Las Vegas, Nevada 89154-4002, and European Synchrotron Radiation Facility, Grenoble, France

When β-nitrous oxide (*Cmca* N₂O) is laser heated to between 2000 and 3400 K at high pressures (10−55 GPa), it disproportionates into an ionic form of dimeric nitrogen dioxide (NO⁺NO₃⁻) and nitrogen. Raman spectra of the quenched products suggest that the ionic phase is stable to 55 GPa at ambient temperature but, upon subsequent heating at pressures below 30 GPa, further dissociates into nitrogen, oxygen, and other nitrogen−oxygen compounds. X-ray diffraction patterns of the ionic phase indicate that it has an orthorhombic structure (Z = 4, ρ_o = 2.69 g/cm³), similar to the aragonite phase of calcium carbonate. The results suggest that the primary driver for ionization is densification at high pressures, whereas dissociation between 10 and 30 GPa results from the combined effects of densification and entropy increases.

Crystal structures and intermolecular interactions of simple molecular solids have well been understood in terms of quadrupole−quadrupole interaction for many decades.[1,2] These weak interactions also make molecular solids relatively soft at low pressures. However, at high pressures, molecular solids rapidly become much denser, and the intermolecular interactions become highly repulsive. This repulsion results in part from a rapid increase in electron kinetic energy at high density, which increases the instability of electrons localized within intramolecular bonds. For this reason, molecular solids often transform at high pressures into molecular configurations and crystal structures with more itinerant electrons and lower energies. The insulator-to-metal transition is a good example of this electron delocalization model, which has long been of interest in condensed matter physics.[3,4] Molecular-to-nonmolecular transitions recently discovered in nitrogen[5,6] and carbon dioxide[7−11] also support the model. In this study, we show yet another mechanism (i.e., ionization) that softens the repulsive potential by the formation of ion pairs in N₂O, a molecular analogue of CO₂.

Nitrous oxide (N₂O) and carbon dioxide (CO₂) are isoelectronic and have similar melting temperatures and crystal structures at moderate pressures. At ambient temperature, N₂O and CO₂ crystallize into an orientation-disordered cubic (*Pa*3) α-phase at around 1 GPa and transform into an ordered orthorhombic (*Cmca*) β-phase at 4 GPa for N₂O and 11 GPa for CO₂.[12,13] The crystal structures of α- and β-N₂O are similar to those of CO₂-I and -III, respectively.[13,14] These room-temperature phases of CO₂ and N₂O are considered to be molecular below 10−20 GPa and are stabilized mainly by quadrupole-quadrupole interactions.[1,2] At higher pressures, CO₂-III develops unusually high lattice strains and strength (above 20 GPa) and transforms into the bent molecular phase IV (at 500−1500 K and 10−35 GPa)[15,16] and the nonmolecular phase

V (above 35 GPa and 1800 K).[7−11] The properties of N₂O, however, are less completely known at comparably high pressures and temperatures (above 12 GPa and ambient temperature). Thus, the systematics of these important linear triatomic molecules are incompletely understood. In this paper, we demonstrate that N₂O disproportionates into a known ionic form of the NO₂ dimer (NO⁺NO₃⁻)[17,18] and nitrogen (N₂) at high pressures and temperatures. We also present X-ray evidence for the crystal structures of β-N₂O and NO⁺NO₃⁻ to 55 GPa and discuss the basis for the stability of this dissociation products.

Liquid N₂O was loaded into a diamond-anvil cell (DAC) contained in an autoclave by condensing gaseous N₂O at 234 K and 1 MPa. A few micron-size ruby chips were scattered inside the cell, providing for in situ determinations of pressures at several locations in the sample. N₂O samples were indirectly heated by irradiating the ruby chips with a Nd:YLF laser (TEM₀₀ at 1054 nm). Temperatures during laser heating were approximately determined by fitting the thermal emission from the laser-heated area to a gray-body radiation formula. The transformation (or ionization) of β-N₂O was typically associated with a bright flash of light, indicating a highly exothermic reaction to new structures that contain ionic species and other products. Because the bright emission is transient, it is difficult to determine the onset temperature for ionization. Therefore, in the present study we only estimate the exothermic reaction temperature (not the ionization temperature) by assuming that all emission is thermal. In contrast to the laser-heating experiments at higher temperatures, external resistive heating of N₂O samples to 800 K at 20 GPa did not induce the ionization in a time scale of hours.

Five samples of β-N₂O were used for laser-heating experiments at pressures between 10 and 55 GPa; two other samples were used for X-ray diffraction for β-N₂O to 50 GPa. The quenched postheating products were characterized by using micro-Raman spectroscopy. Crystal structures of the quenched phases were determined by angle-resolved X-ray diffraction using focused monochromatic (λ = 0.3738 Å) X-rays at the

---
* Corresponding author.
[†] Lawrence Livermore National Laboratory.
[‡] University of Nevada Las Vegas.
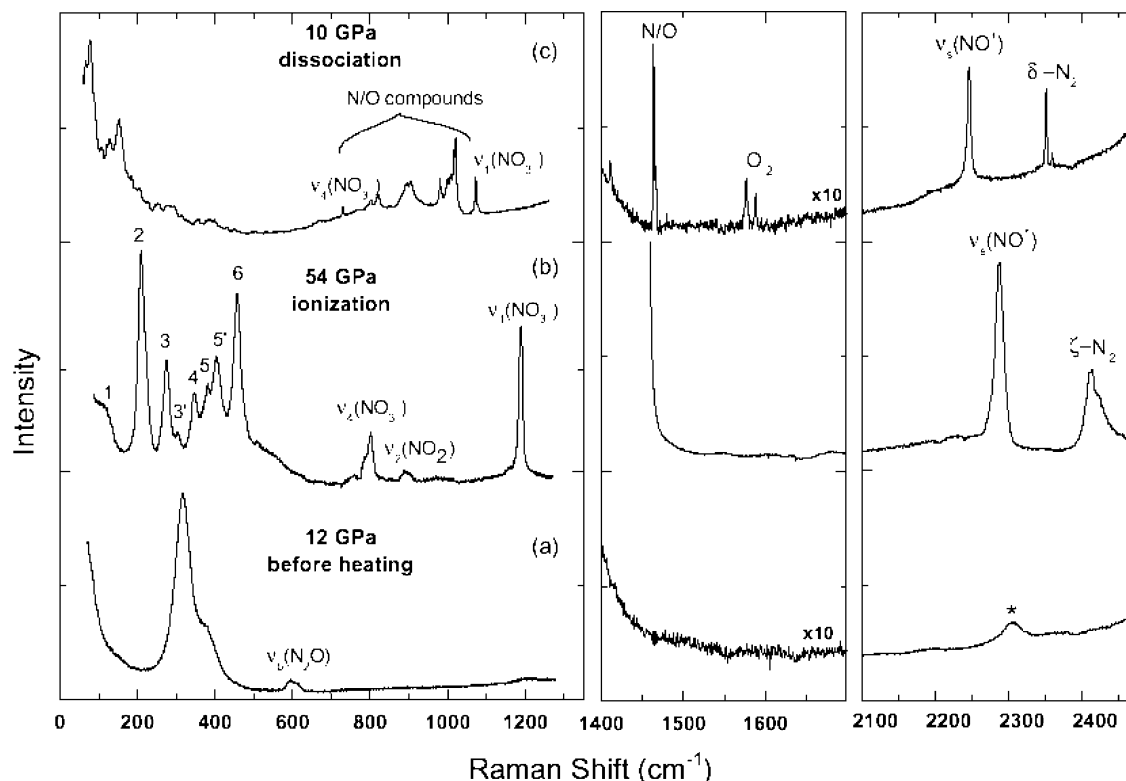[§] European Synchrotron Radiation Facility.

Disproportionation and Transformations of N$_2$O

J. Phys. Chem. B, Vol. 107, No. 24, 2003 **5923**

Figure 1. Raman spectra of β-N$_2$O (a) before and (b, c) after laser-heating, showing the pressure-induced reactions to (b) the ionization products of NO$^+$NO$_3^-$ and η-N$_2$ at 54 GPa and (c) the dissociation products δ-N$_2$ containing dissolved O$_2$, N/O-compounds, and NO$^+$NO$_3^-$ at 10 GPa.

European Synchrotron Radiation Facility. The diffraction patterns were recorded on a high-resolution image-plate detector (MAR2500) and were analyzed by using the FIT2D program.[19]

Raman spectra of the sample before and after laser-heating to 2840 K at 54 GPa (Figure 1) indicate that β-N$_2$O disproportionates into an ionic nitrogen dioxide dimer, NO$^+$NO$_3^-$ or nitrosonium nitrate, and δ-N$_2$. The broad features between 200 and 400 cm^{-1} before heating (Figure 1a) are characteristic of β-N$_2$O. Before heating, the spectrum changes with pressure only slightly; all bands shift slightly toward higher frequencies as the pressure increases. However, the Raman spectra measured after laser heating (Figure 1b,c) markedly differ from spectra characteristic of two molecular polymorphs, α- and β-N$_2$O. The features at 1180 and 795 cm^{-1} in Figure 1b are characteristic for two Raman-active stretching ν_1 (A′) and bending ν_4 (E′) modes of the nitrate ion (NO$_3^-$). The most dominant feature at 2275 cm^{-1} is the symmetric stretching, ν_s(A$_g$), of the nitrosonium ion (NO$^+$). The frequencies of these modes extrapolated to the ambient pressure (Figure 2) are in excellent agreement with those previously observed in NO$^+$NO$_3^-$ both at low temperature at ambient pressure[17] and at high temperature at high pressure.[18] A weak feature at 850 cm^{-1} is probably a bending vibration ν_2(A$_g$) mode of NO$_2$ arising from a minor molecular product of N$_2$O$_4$.[18] The features between 2400 and 2450 cm^{-1} are also characteristic of the stretching modes of ζ-N$_2$.[20]

Laser-heating of β-N$_2$O at lower pressures, 10−20 GPa, to about 2000 K (Figure 1c) produces a more complicated set of products, consisting of δ-N$_2$ (the doublet near 2365 cm^{-1}), β-O$_2$ (doublet at 1650 cm^{-1}), NO$^+$NO$_3^-$ (730, 835, 1095, and 2250 cm^{-1}), and other nitrogen−oxygen products (features between 750 and 1070 cm^{-1}). Subsequent heating of the ionic product at pressures below 30 GPa also produces a complex set of dissociation products. We conclude, therefore, that the ionic phase NO$^+$NO$_3^-$ further dissociates into N$_2$ and O$_2$. In fact,
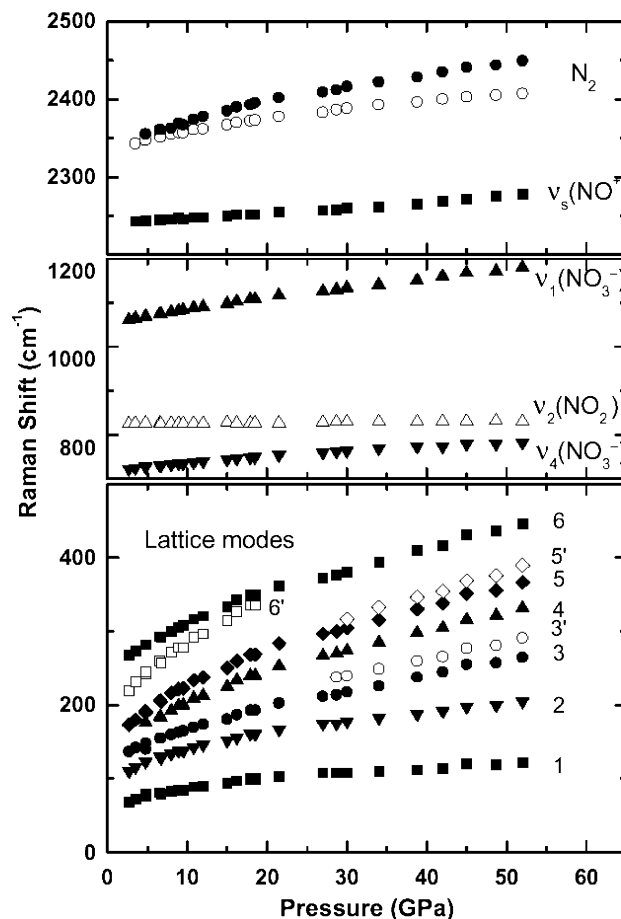

Figure 2. Pressure-induced shifts of the vibrational Raman modes of the ionic product, NO$^+$NO$_3^-$, and of N$_2$.

the ionization is always accompanied by dissociation when β-N$_2$O is laser-heated at pressures below 30 GPa, whereas no

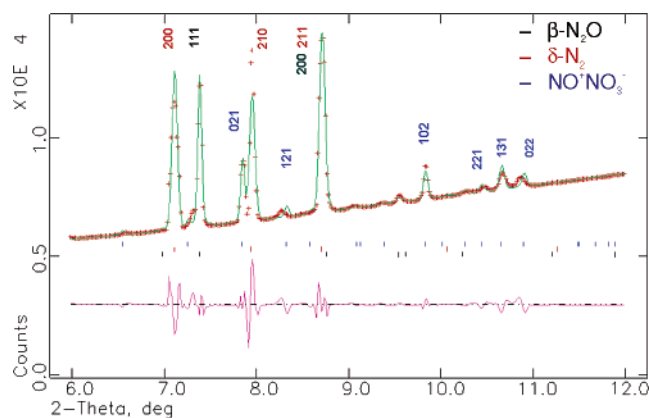**Figure 3.** X-ray diffraction pattern of the ionic products measured at 7 GPa (red cross), showing the reflections from δ-N_2, β-N_2O, and $NO^+NO_3^-$. The calculated diffraction of the mixture (green line) is overlaid on the measured diffraction (red crosses). Below the patterns, the Bragg peak positions are marked in vertical bars for $NO^+NO_3^-$ (top in blue), δ-N_2 (middle in red), and β-N_2O (bottom in black), together with the difference spectrum (pink line) between the calculated and observed diffraction patterns. Indices are included for several features. This sample was synthesized at 35 GPa to avoid the dissociation (see text).

evidence for further dissociation of $NO^+NO_3^-$ was observed to 3370 K at higher pressures. These results suggest that the dissociation temperature of the ionic dimer increases with increasing pressure. Note also in Figure 1c the splitting of the oxygen stretching mode, indicating that the oxygen is dissolved in δ-N_2 ($Pm3n$).[21] This splitting is due to a vibration-vibration resonance transfer between molecules at two types of molecular sites of δ-N_2.[22] The relative intensities of the components of the doublet vary with pressure and composition,[21] on which basis we estimate the oxygen content of the δ-N_2 in Figure 1c to be about 10%.

The products of both the ionic and dissociation reactions (Figure 1b,c, respectively) can be quenched to room temperature at all pressures studied (between 10 and 55 GPa). Because of the complexity and ill-defined chemistries of the nitrogen−oxygen dissociation products, we only characterize the pressure dependence of the ionic products. The ionic phase ($NO^+NO_3^-$) is stable in a wide pressure region to 55 GPa, the maximum pressure applied (Figure 2). No reverse transition of $NO^+NO_3^-$ to the molecular phases of N_2O_4, N_2O, or NO_2 was observed even below the α/β-N_2O transition pressure, 4 GPa. This behavior differs from those of the high pressure−temperature phases of CO_2 (phases II, III, IV, and V and its ionic dimer phase[23]), all of which transform back to phase I ($Pa3$) near 11 GPa[16] at ambient temperature and from results reported elsewhere.[24] Note that the splitting of the ν_4 mode of $NO^+NO_3^-$ above 35 GPa probably resulted from the anisotropic strain developed in the lattice.

The crystal structures of β-N_2O and $NO^+NO_3^-$ have been characterized to 55 GPa at ambient temperature. Diffraction patterns of β-N_2O before heating easily fit to the known structure: the orthorhombic $Cmca$ cell with $Z = 4$.[13] In this structure, all N_2O molecules are aligned parallel to the bc-basal plane with their molecular axes tilted by about 37° from the c-axis.[13] X-ray diffraction patterns of the quenched ionic product (Figure 3), on the other hand, consists of reflections from δ-N_2 ($Pm3n$), β-N_2O ($Cmca$), and $NO^+NO_3^-$. The X-ray intensity data with highly preferred orientations, however, do not allow rigorous refinement of crystal structures for all products. Nevertheless, on the basis of a Le Bail fit of the mixture, we found a reasonable description of the observed X-ray diffraction,
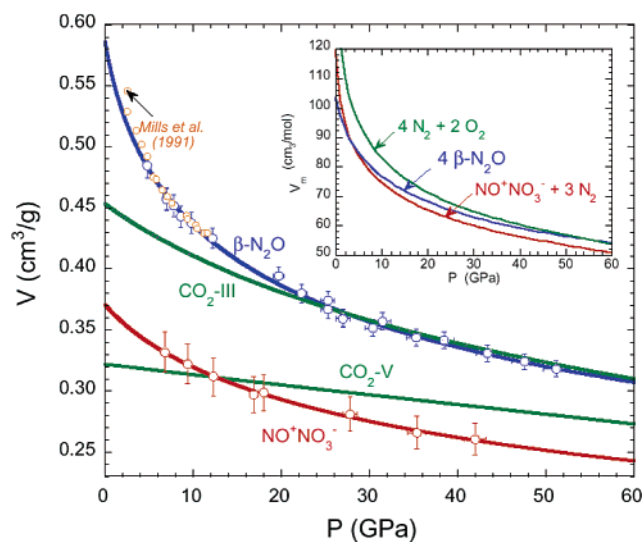

Figure 4. Isotherms of β-N_2O and $NO^+NO_3^-$, at ambient temperature compared with those of CO_2-III, CO_2-V, and δ-N_2. The inset compares the molar volumes of 4 β-N_2O and $NO^+NO_3^-$ + 3 δ-N_2, illustrating that densification is responsible for the ionization of β-N_2O above 5 GPa.

as shown in Figure 3. The calculated X-ray diffraction pattern consists of diffraction lines from β-N_2O ($Cmca$; $a = 4.891$ Å, $b = 4.465$ Å, $c = 6.138$ Å), δ-N_2 ($Pm3n$; $a = 6.027$ Å), and an orthorhombic structure with the lattice parameters $a = 5.923$ Å, $b = 7.255$ Å, and $c = 4.717$ Å. Note that the systematic extinctions of the orthorhombic cell are consistent with either $Pnma$ or $Pn2_1a$. Further structural refinement of this new phase was not attempted because its orientation is highly preferred and it is a minority in the mixture. However, it is noteworthy that the $Pnma$ structure is analogous to aragonite, $CaCO_3$, which structure also occurs in other nitrates, e.g., KNO_3 or NH_3NO_3.[25]

Figure 4 compares room-temperature isotherms for β-N_2O and $NO^+NO_3^-$ to 55 GPa with those of CO_2-III and CO_2-V. The present data for β-N_2O (blue circles to 50 GPa with error bars) are in good agreement with the previous data (red circles between 4 and 12 GPa).[13] Note that the previous data below 4 GPa are for α-N_2O ($Pa3$), whose specific volume is slightly larger than that of β-N_2O. To 15 GPa, β-N_2O is relatively soft initially ($B_o = 10.9$ GPa), as is typical of molecular solids, e.g., α-N_2O ($B_o = 7.9$) and CO_2-I ($B_o = 6.2$). At higher pressures, β-N_2O rapidly stiffens, and its compression curve becomes essentially identical to that of CO_2-III ($B_o = 87$ GPa).[9] In fact, above 20 GPa, β-N_2O samples even develop textures typical of highly strained lattices, which were previously observed for CO_2-III.[9]

The ionic phase of $NO^+NO_3^-$ behaves quite differently from the nonmolecular phase CO_2-V. $NO^+NO_3^-$ is substantially softer ($B_o = 45.0$ GPa) than polymeric CO_2-V ($B_o = 362$ GPa).[9] As a result, $NO^+NO_3^-$ becomes denser than CO_2-V above 12 GPa despite its lower density at ambient pressure. The higher density of $NO^+NO_3^-$ than CO_2-V at high pressures probably reflects a more efficient packing of the ion pairs in $NO^+NO_3^-$ than the packing of atoms in a tetrahedral network structure, CO_2-V. This higher packing is probably due to relatively strong attractive Coulombic interactions among ion pairs, in contrast to very stiff covalent bonds of CO_2-V with its low-coordination structure. This result is also consistent with the higher number of nearest neighbors in $NO^+NO_3^-$ than CO_2-V; for example, each nitrosonium (NO^+) ion has six nearest nitrate ions,[25] whereas each carbon atom in CO_2-V has only four nearest oxygen atoms.[9]

The inset of Figure 4 compares the molar volumes of β-N_2O with the ionic and dissociation products. Above 5 GPa, the mixture of $NO^+NO_3^-$ and N_2[26] has the smallest molar volume and thus is favored over both β-N_2O and the two moles of solid N_2 and one of O_2 or a reasonable mixture of these two.[27] On the other hand, the molar volume of a reasonable N_2–O_2 mixture becomes smaller than that of β-N_2O above 56 GPa and, based on the extrapolation, of $NO^+NO_3^-$ above 130 GPa. This result thus suggests that the ionization is primarily driven by densification at high pressures, whereas the dissociation observed between 10 and 30 GPa results from the combined effects of densification and entropy increase at high pressures and temperatures. This conclusion is also consistent with the presumption that the dissociation would require higher temperature than the ionization.

Although we have produced an ionic dimer of carbon dioxide by combustion of various forms of carbon at high temperatures and pressures less than 20 GPa,[28] no molecular dimer equivalent to N_2O_4 has been found in the CO_2 system. We suggest, therefore, that differences of high-temperature, high-pressure reactivities between N_2O and CO_2 derives from the facile molecular dissociation channels of N_2O to N_2, $(NO)_2$, and N_2O_4 that are neither kinetically nor thermodynamically accessible in the CO_2 system.

In summary, although the multiple bonds in both N_2O and CO_2 become unstable at high pressures, the electron richness of nitrogen precludes the formation of extended N–O bonds for β-N_2O even at 50 GPa. At this pressure, the intermolecular N–O distance ($\sim$2.44 Å) becomes substantially less than twice the N–O single bond distance of NO_3^- ($\sim$1.36 Å), certainly within the domain of highly repulsive interaction (for comparison, CO_2-III transforms into the extended phase V at a substantially greater C–O distance $\sim$2.52 Å). Instead, β-N_2O disproportionates into an ionic solid $NO^+NO_3^-$ and nitrogen to soften the repulsive potential by strong Coulombic interactions between the ionic pairs. Such ionic attractions draw the ion pairs even closer to produce a higher density solid. Finally, the contrast observed in the present study between the pressure-induced changes of CO_2 and N_2O is analogous to that previously observed in another isoelectronic pair, N_2[5,6] and CO,[29] at high pressures.

References and Notes

(1) English, C. A.; Venables, J. A. *Proc. R. Soc. London A* **1974**, *340*, 57.

(2) Kuchta, B.; Etters, R. D. *J. Chem. Phys.* **1991**, *95*, 5399.

(3) Weir, S. T.; Mitchell, A. C.; Nellis, W. J. *Phys. Rev. Lett.* **1996**, *76*, 1860.

(4) Desgreniers, S.; Vohra, Y. K.; Ruoff, A. L. *J. Phys. Chem.* **1990**, *94*, 1117.

(5) Goncharov, A. F.; Gregoryanz, E.; Mao, H. K.; Liu, Z.; Hemley, R. J. *Phys. Rev. Lett.* **2000**, *85*, 1262.

(6) Erements, M. L.; Hemley, R. J.; Mao, H. K.; Gregoryanz, E. *Nature* **2001**, *411*, 170.

(7) Iota, V.; Yoo, C. S.; Cynn, H. *Science* **1998**, *283*, 1510.

(8) Serre, S.; Cavazzoni, C.; Chiarotti, G. L.; Scandolo, S.; Tosatti, E. *Science* **1999**, *284*, 788.

(9) Yoo, C. S.; Cynn, H.; Gygi, F.; Galli, G.; Iota, V.; Nicol, M.; Carlson, S.; Hauserman, D.; Mailhiot, C. *Phys. Rev. Lett.* **1999**, *83*, 5527.

(10) Dong, J.; Tomfohr, J. K.; Sankey, O. F. *Phys. Rev. B* **2000**, *61*, 5967.

(11) Holm, B.; Ahuja, R.; Belomoshko, A.; Johansson, B. *Phys. Rev. Lett.* **2000**, *85*, 1258.

(12) Olijnyk, H.; Daufer, H.; Jodl, H.-J. *J. Chem. Phys.* **1988**, 88, 4204. Olijnyk, H.; Jephcoat, A. P. *Phys. Rev. B* **1998**, *57*, 879.

(13) Mills, R. L.; Olinger, B.; Cromer, D. T.; LeSar, R. *J. Chem. Phys.* **1991**, *95*, 5392.

(14) Aoki, K.; Yamawaki, H.; Sakashita, M.; Gotoh, Y.; Takemur, K. *Science* **1994**, *263*, 356.

(15) Yoo, C. S.; Iota, V.; Cynn, H. *Phys. Rev. Lett.* **2001**, *86*, 444.

(16) Iota, V.; Yoo, C. S. *Phys. Rev. Lett.* **2001**, *86*, 5922.

(17) Bolduan, F.; Jodl, H. J.; Loewenschuss, A. *J. Chem. Phys.* **1984**, *80*, 1739.

(18) Agnew, S. F.; Swanson, B. I.; Jones, L. H.; Mills, R. L.; Schiferl, D. *J. Phys. Chem.* **1983**, *87*, 5065.

(19) Hammersley, A. P. FIT2D V9.129 Reference manual v3.1; ESRF report 98HA01T, 1998.

(20) Bini, R.; Ulivi, L.; Kreutz, J.; Jodl, H.-J. *J. Chem. Phys.* **2000**, *112*, 8522.

(21) Baer, B.; Nicol, M. *J. Phys. Chem.* **1990**, *94*, 1073.

(22) Cromer, D. T.; Mills, R. L.; Schiferl, D.; Schwalbe, L. A. *Acta Crystallogr. B* **1981**, *37*, 8.

(23) Yoo, C. S. *Science and Technology of High Pressure*; Manghnani, M. H., Nellis, W., Nicol, M. F., Eds.; University Press: Hyberadad, India, 2000; Vol. 1, p 86.

(24) Somayazulu, M.; Madduri, A.; Goncharov, A. F.; Tschauner, O.; McMillan, P. F.; Mao, H. K.; Hemley, R. J. *Phys. Rev. Lett.* **2001**, *87*, 135504.

(25) Wyckoff, R. W. G. *Crystal Structures*, 2nd ed.; John Wiley & Sons: New York, 1964; Vol. 2, Chapter VII.

(26) Hanfland, M.; Lorenzen, M.; Wassilew-Reul, C.; Zontone, F. *Rev. High Press. Sci. Technol.* **1998**, *7*, 787 Also see the ESRF web page by M. Hanfland, 2000.

(27) Akahama, Y.; Kawamura, H.; Haeusermann, D.; Hanfland, M. *Phys. Rev. Lett.* **1995**, *74*, 4690.

(28) Yoo, C. S.; Cynn, H.; Nicol, M. Unpublished results.

(29) Katz, A. I.; Schiferl, D.; Mills, R. L. *J. Phys. Chem.* **1984**, *88*, 3176.